Int. J. Electrochem. Sci., 17 **(2022)** Article Number: 220449, doi: 10.20964/2022.04.37

International Journal of
ELECTROCHEMICAL
SCIENCE
www.electrochemsci.org

Mini review

Progress in nanomaterials-based electrochemical biosensors for the detection of interleukins

Lingbin Ou [1,*] *and Ning Xia* [2,*]

[1] School of Medical Technology, Yongzhou Vocational Technical College, Yongzhou 425100, Hunan, China
[2] Henan Province of Key Laboratory of New Optoelectronic Functional Materials, Anyang Normal University, Anyang 455000, Henan, China
[*]E-mail: xiaobinxuer@163.com (L.O.); xianing82414@163.com (N.X.)

Received: 17 December 2021 / *Accepted:* 16 January 2022 / *Published:* 4 March 2022

Interleukins (ILs) are closely related to the occurrence and progress of many diseases including neuropsychiatric syndrome and Crohn's disease. Therefore, it is of great importance to determining ILs for the early diagnosis and treatment of diseases. Electrochemical biosensors are the promising candidates for the sensitive and specific detection of ultra-low level of biomarkers. This review summarized the development of nanomaterials-based electrochemical biosensors for ILs detection. It was highlighted that the utilization of nanomaterials as the electrode materials and the signal reporters or carriers for the construction of electrochemical biosensors.

Keywords: Interleukins; electrochemical biosensor; nanomaterials; electrode materials; signal amplification

1. INTRODUCTION

Crohn's disease is a chronic granulomatous inflammatory disease in the whole intestinal tract. It is mainly characterized by T cell activation and inflammatory cell aggregation in the mucosa. At present, the methods for diagnosis of Crohn's disease mainly include colonoscopy, X-ray barium enema and systematic barium meal examination [1]. However, all of them are invasive and not suitable for some special patients, such as intestinal obstruction, fulminant or severe patients.

Cytokines can aggravate and persist inflammation through a variety of different mechanisms, and eventually cause chronic injury to intestinal tissue. Detection of cytokines in body fluids is of great significance for the diagnosis and progress of Crohn's disease [2]. Interleukins (ILs), a kind of cytokines, are produced by many kinds of cells. They play an important role in transmitting information, activating

and regulating immune cells, mediating the activation, proliferation and differentiation of cells [3]. At present, enzyme-linked immunosorbent assay (ELISA) is the standard method for ILs detection in clinic. However, the method often faces some inherent shortcomings, such as time-consuming, labor-intensive and low sensitivity. To detect ultra-low level of ILs in body fluids, various novel platforms have been exploited, including fluorescence, colorimetry, surface plasmon resonance, surface enhanced Raman scattering and electrochemistry [4-6]. Among them, electrochemical biosensors have attracted much attention because of their remarkable advantages of high selectivity, rapid response, low cost and easy operation [7, 8]. In particular, the progress of nanotechnology has promoted the development of electrochemical biosensors with high sensitivity and selectivity. In this review, nanomaterial-based electrochemical platforms were discussed for the determination of different ILs in a direct or sandwich-type detection format. The analytical performances of the two types of electrochemical biosensors are included in Table 1 and 2.

2. DIRECT DETECTION

As a key component of electrochemical devices, electrodes play a critical effect on the performances of biosensors. Different types of electrodes have been made for electrochemical assays, including glass carbon electrode, carbon paste electrode, metal/metal oxide electrode and so on. Besides, various materials have been utilized to modify the electrode, aiming to facilitate the immobilization of biorecognition elements (antibodies and aptamers) and/or accelerating the electron communication between redox mediators and electrode surface. When being captured by antibody anchored on the electrode, antigen can hamper the electron transfer and lead to the detectable change of electrochemical features of electrode interfaces. These electrode-electrolyte interfacial molecular coupling events can be label-free and directly monitored by different electrochemical techniques, such as electrochemical impedance spectroscopy (EIS) and voltammetry [9].

The formation of SAMs is a popular and convenient technique to functionalize the electrode for the subsequent immobilization of antibody. The selection of chemicals with appropriate groups is dependent upon the type of electrode surface [10]. For example, Aydın et al. used 6-phosphonohexanoic acid (PHA) to modify indium tin oxide electrode (ITO) for the immobilization of two different antibodies, which allowed for the detection of interleukin-1 (IL-1) and interleukin-8 (IL-8) by EIS [11, 12]. Sharma et al. functionalized the gold electrode (AuE) with monothiol-alkane PEG-COOH SAMs for IL-8 detection with sub-pg/mL sensitivity [13]. 3-(Triethoxysilyl) propyl isocyanate with isocyanate groups were utilized to decorate cost-effective fluorine tin oxide electrode for IL-8 detection [14]. Gentili et al. employed (11-mercaptoundecyl)hexa(ethylene glycol) acetic acid terminated (EG_6COOH) to modify gold gate electrode for IL-6 detection [15]. To improve the conductivity and surface area, a series of conducting polymers have been used for the modification of electrode, including polythiophene and polypyrole [16-21]. Typically, the conjugated poly(pyrrole N-hydroxy succinimide) polymers were used to produce SAMs on ITO, in which a number of succinimide groups in the polymers were further labeled with antibodies to determine IL-6 in human serum [22]. Moreover, Cardoso et al. utilized ploy(3,4-ethylenedioxythiophene) as the substrate to form molecularly imprinted polymer on a screen-printed carbon electrode for IL-1 detection [23].

Nowadays, a variety of nanomaterials have been extensively utilized as the functionalized materials to modify the sensor electrode, such as carbon-based nanomaterials, metal nanoparticles (NPs), polymeric nanomaterials, magnetic NPs and nanohybrids. The excellent merits of large surface area-volume ratio, enhanced electronic conductivity, superior catalytic activity and rapid electrode kinetics endow electrochemical biosensors with faster electron transfer rate, higher sensitivity and lower detection limit [24, 25]. Besides, biocompatible nanomaterials favor the robust attachment of a large amount of biorecognition elements and improve the accessibility of targets to the receptors.

Carbon-based nanomaterials, such as graphene and carbon nanotubes, have been intensively utilized in the field of electrochemical sensors, owing to their unique chemical and physical properties [26]. Parate et al. proposed an aerosol-jet-printed (AJP) graphene immunosensor for the label-free determination of IL-10 in serum [27]. As displayed in Figure 1, graphene was synthesized through facile liquid-phase exfoliation of graphite. The obtained graphene dispersion with nitrocellulose was used as the ink to prepare flexible AJP graphene electrode with high spatial resolution. Then, interdigitated electrodes (IDEs) were treated with thermally annealing in a CO_2 environment to generate surface carboxyl groups for the immobilization of antibodies. The immunosensor could monitor cytokines (interferon gamma (IFN-γ) and IL-10) in serum with wide linear ranges.

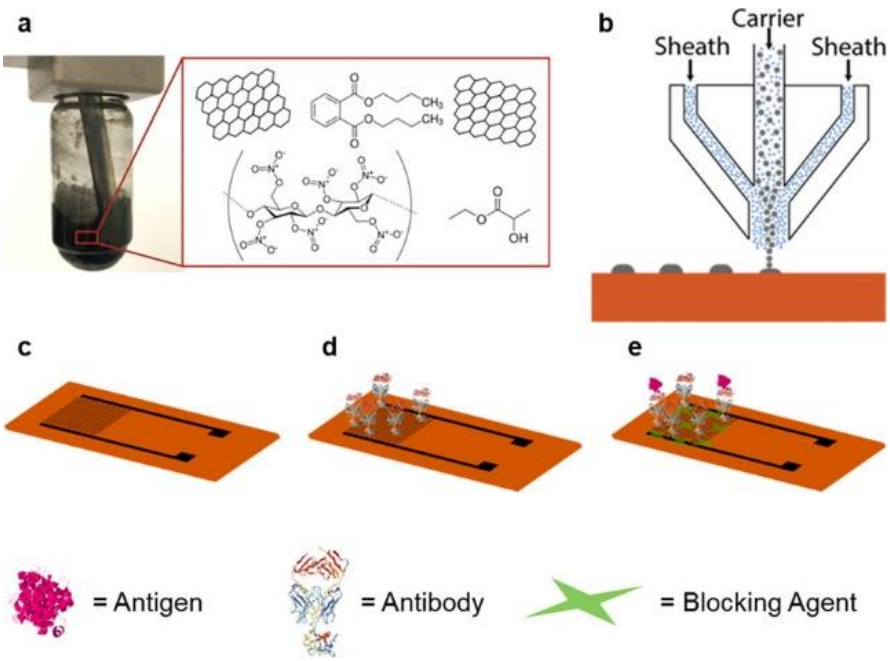

Figure 1. Schematic representation of fabrication and biofunctionalization of the AJP graphene IDE. (a) Schematic demonstrating the graphene ink formulation for aerosol printing. (b) Aerosol jet printing mechanism of the graphene ink illustrating a sheath gas enveloping the carrier flow of aerosolized graphene ink particles for focusing the ink to a desired diameter. (c) AJP graphene IDE on a polyimide (Kapton) sheet. (d) Antibodies selective to IL-10 or IFN-γ are immobilized on the carboxyl group functionalized graphene surface using N-(3-dimethylaminopropyl)-N'-ethylcarbodiimide/N-hydroxysuccinimide (EDC/NHS) chemistry. (e) The remaining exposed surface of the graphene sensor is covered with the blocking agent (mixture of bovine serum albumin (BSA), fish gelatin, and Tween-20) and incubated with antigen. [27]. Copyright 2020 American Chemical Society.

Gold nanoparticles (AuNPs) were also particularly popular in the electrochemical fields due to their simple preparation process and ease of functionalization. Tertis et al. used conductive polypyrrole NPs and AuNPs to modify screen-printed graphite electrode for the immobilization of aptamers and the label-free assay of IL-6 [28]. For the covalent immobilization of AuNPs on the electrode, *p*-aminobenzoic acid film was first electrochemically grafted on the electrode and then derivated with *p*-paminothiophenol to provide thiol groups for anchoring of AuNPs [29]. Transition metal-based molybdates can also be utilized as the substrates for the development of biosensors. Pachauri et al. reported a silver molybdate nanoparticles (β-Ag_2MoO_4 NPs)-based immunosensor for analysis of IL-8 [30]. Besides, nanohybrids have received more attention in electrochemical biosensors thanks to the synergetic effect [31]. Verma et al. developed an immunosensing platform for electrochemical detection of IL-8 using AuNPs-reduced graphene oxide (AuNPs-rGO) nanocomposites as the transducer matrixes [32]. As presented in Figure 2, rGO was in-situ decorated with AuNPs to improve the electronic and electrochemical properties. The carboxylic group of AuNPs-rGO nanocomposites on the ITO surface were linked to the amine groups of antibodies through the covalent interactions. The effect of antibody-antigen binding on the electrolyte/channel interface was monitored by differential pulse voltammetry (DPV). Recently, Liu et al. reported a wrinkled SiO_2 NPs-assisted sacrificing strategy to synthesize hierarchical nanoporous mesoporous-carbon (NMC) that could load more nanoparticles to enhance the sample enrichment [33].

Table 1. Analytical performances of various sensing electrodes for interleukins detection.

Electrode Modifier	**Target**	**Detection limit (fg/mL)**	**Linear range (ng/mL)**	**Ref.**
PHP	IL-1	6	2×10^{-5} ~ 2×10^{-3}	[10]
PHA	IL-1	7.5	2.5×10^{-5} ~ 3×10^{-3}	[11]
PHA	IL-8	6	2×10^{-5} ~ 3×10^{-3}	[12]
monothiol-alkane PEG-COOH	IL-8	90	9×10^{-3} ~ 9×10^{2}	[13]
3-(triethoxysilyl) propyl isocyanate	IL-8	11.9	2×10^{-5} ~ 4×10^{-3}	[14]
poly(2-thiophen-3-yl-malonic acid)	IL-1	3	1×10^{-5} ~ 3×10^{-3}	[16]
poly(1-(2-cyanoethyl)pyrrole)	IL-6	360	1×10^{-3} ~ 5×10^{-2}	[17]
polypyrole	IL-6	6	2×10^{-5} ~ 1.6×10^{-2}	[18]
polypyrole	IL-10	347	1×10^{-3} ~ 1×10^{-2}	[19]
epoxy-substituted-polypyrrole	IL-6	3.2	1×10^{-5} ~ 5×10^{-2}	[20]
polypyrole	IL-6	20	2×10^{-5} ~ 2×10^{3}	[21]
PPyr-NHS	IL-6	10.2	3×10^{-5} ~ 2.25×10^{-2}	[22]
PEDOT/4-aminothiophenol	IL-1	1.6 pM	60 pM ~ 600 nM	[23]
Au NPs-Thi-CMWCNTs	IL-6	2.87×10^{3}	0.01 ~ 800	[26]
Graphene	IL-10	4.6×10^{4}	0.1 ~ 2	[27]
polypyrrole NPs and AuNPs	IL-6	330	1×10^{-3} ~ 1.5×10^{4}	[28]
AuNPs	IL-6	1.6×10^{3}	5×10^{-3} ~ 100	[29]
β-Ag_2MoO_4 NPs	IL-8	9×10^{4}	1×10^{-6} ~ 40	[30]

SWCNTs-AuNPs	IL-6	0.01	1×10^{-8} ~ 1×10^{-4}	[31]
AuNPs-rGO	IL-8	7.273×10^{4}	5×10^{-4} ~ 4	[32]
NMC-AuNPs	IL-6	140	5×10^{-4} ~ 1.2	[33]

Abbreviation: PHP, 3-phosphonopropionic acid; PHA, 6-phosphonohexanoic acid, PPyr-NHS, poly(pyrrole N-hydroxy succinimide); PEDOT, ploy(3,4-ethylenedioxythiophene); AuNPs, gold nanoparticles; Thi, thionine; CMWCNTs, carboxylated multi walled carbon nanotubes; NPs, nanoparticles; SWCNTs, single-walled carbon nanotube; rGO, reduced graphene oxide; NMC, nanoporous mesoporous-carbon.

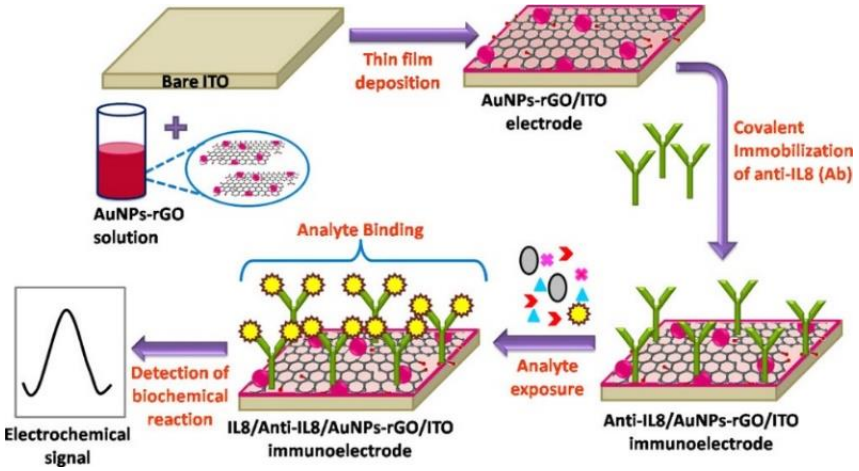

Figure 2. Schematic of fabrication of AuNPs-rGO-based immunoelectrode for immunosensing application [32]. Copyright 2017 American Chemical Society.

3. SANDWICH-TYPE DETECTION

Despite of the simplicity and low cost, the low sensitivity heavily limited the applications of the direct detection methods. To improve the sensitivity, nanomaterials-based signal amplification strategies have been integrated into the electrochemical assays. Usually, nanomaterials can be used as the carriers of enzymes or redox reporters and the signal markers for sandwich assays of targets.

3.1 Nanomaterials as the carriers

During the traditional sandwich-type bioassays, one target can only bind with one reporter, leading to the limited signal [34]. Therefore, multienzyme-based signal amplification strategies were designed for the development of ultrasensitive electrochemical biosensors. For instance, Wang et al. reported a supersandwich multienzyme-DNA label-based electrochemical immunosensor for IL-6 detection [35]. In this work, the biotinylated secondary antibody was first labeled with avidin-terminated sequence 1 (S1) and then S1 was reacted with horseradish peroxidase (HRP)-labeled sequence 2 and 3, eventually generating a supersandwich multienzyme-DNA label. The strong and specific complexation of biotin and avidin is a popular way to form polyenzyme as the catalytic label. For this view, Bhatia et al. developed an electrochemical biosensor for IL-8 detection using a polyenzyme label consisted of biotinylated diaphorase and neutravidin [36].

Noncovalent or covalent conjugation of multienzyme on nanomaterials has been intensively employed in bioassays, such as AuNPs and carbon nanotubes (CNTs). Malhotra et al. reported an electrochemical immunosensor for IL-6 detection by two multienzyme-based signal amplification approaches (Figure 3) [37]. In this work, single-wall carbon nanotube (SWCNT) forests were assembled on pyrolytic graphite electrode for the modification of capture antibody. In the first strategy, the detection antibody-biotin-streptavidin-HRP complex was used as the signal label. In the second method, multiwall carbon nanotube (MWCNT) was used to carry HRP and detection antibody. It was found that the two approaches can measure IL-6 within a broad concentration range. Besides, to improve the electron transfer, AuNPs have been in-situ synthesized on the surface of polydopamine (PDA)-coated CNTs to load HRP and antibody [38]. Magnetic beads (MBs) were used to load enzyme and antibody for signal amplification [39]. Moreover, under the magnetic separation, a low concentration of targets can be enriched and further detected. Malhotra et al. developed a nanostructured microfluidic array for ultrasensitive and simultaneous detection of various cancer biomarkers based on HRP-labeled MBs [40]. As shown in Figure 4, glutathione-capped AuNPs were used to modify the microchannel interface for the immobilization of capture antibody (Ab_1). It was estimated that one MB particle could load 3.9×10^5 HRP molecules and 1.2×10^5 detection antibodies (Ab_2). After the capture of antigens and washing to avoid the non-specific adsorption, MBs were separated and injected into the array for the sensitive detection. In addition, different catalytic enzymes can be loaded on nanomaterials for the cascade reactions. For instance, octahedral anatase TiO_2 mesocrystals (OAMs) were employed to carry acid phosphatase (ACP) and HRP [41]. After the immunoreaction, ACP catalyzed the hydrolysis of 1-naphthyl phosphate into 1-naphthol that was further oxidized by H_2O_2 under the catalysis of HRP.

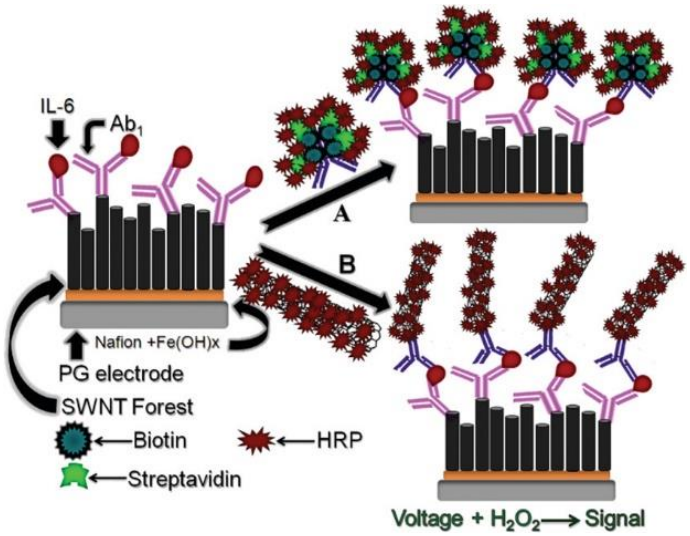

Figure 3. Schematic of two strategies for multilabel detection in the amperometric immunosensor: (A) immunosensor after treating with Ab_2-biotinstreptavidin-HRP, providing 14-16 HRPs on one Ab_2; (B) immunosensor after treating with HRP-MWNT-Ab_2 bioconjugate having 106 active HRPs (enzyme labels) per 100 nm of carboxylated carbon nanotubes. The final detection step involves immersing the immunosensor in an electrochemical cell containing PBS buffer and mediator, applying voltage, and injecting a small amount of hydrogen peroxide [37]. Copyright 2010 American Chemical Society.

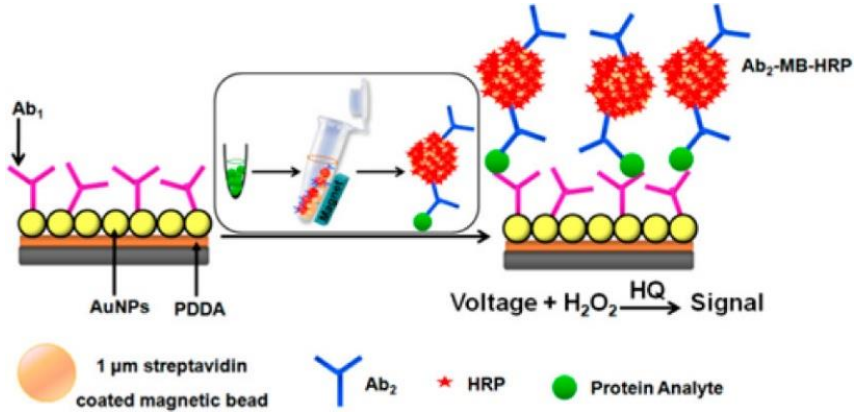

Figure 4. Schematic of the strategy for ultrasensitive amperometric detection by microfluidic immunoarray [40]. Copyright 2012 American Chemical Society.

Electroactive molecules (such as ferrocene and thionine) and ions can be loaded into or onto nanomaterials to produce remarkable signals [42]. For example, Li et al. used $CaCO_3$-templated porous polyelectrolyte NPs to load ferrocene molecules for the determination of IL-6 [43]. Qi et al. reported a label-free electrochemical nanosandwich device for the detection of IL-6 using graphene oxide to carry the redox probe Nile blue (NB) [44]. As shown in Figure 5, AuE was derived with 4-nitrophenyl and then covalently modified with a single layer of GO for the immobilization of Ab_1. Meanwhile, GO acted as a nanoprobe to load a large number of NB molecules for further signal amplification. Jiang et al. employed Cd^{2+}-doped polystyrene sphere (Cd^{2+}-PS) as the label for the detection of IL-17 [45]. After the dissolution of the label by tetrahydrofuran, the contained Cd^{2+} ions were released and then determined by anodic stripping voltammetry (ASV). They also used Cd^{2+}-PS and Fc-PS for the simultaneous detection of IL-6 and IL-17 [46]. Moreover, silver nanoparticles can be loaded on the surface of nanomaterials as signal labels [47]. Shi et al. applied PS@PDA/Cd^{2+} and PS@PDA/AgNPs as the probes to determine IL-6 and matrix metallopeptidase-9 (MMP-9) [48].

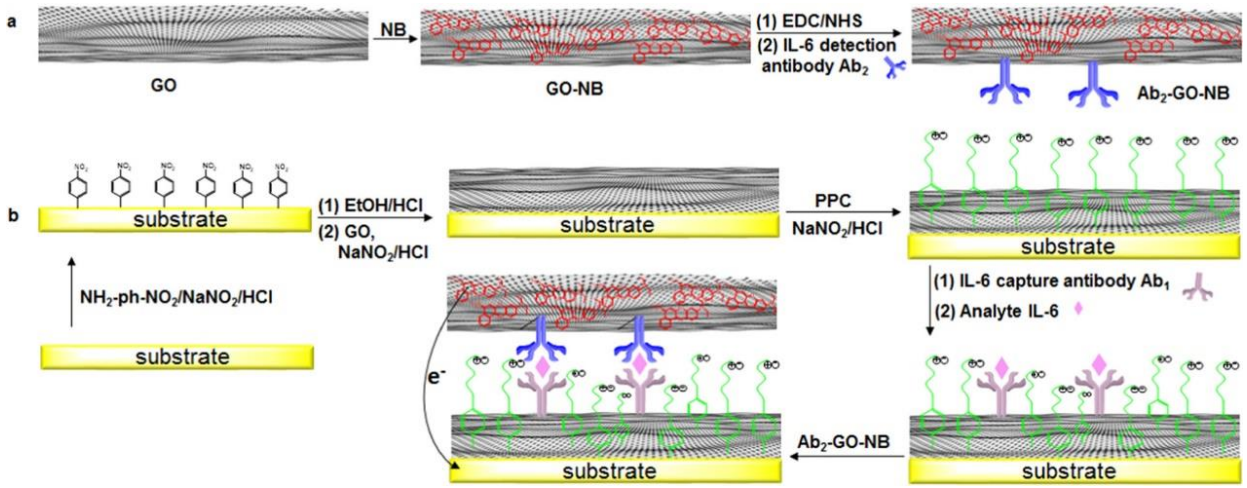

Figure 5. (a) Schematics of the preparation of Ab_2-GO-NB conjugates; (b) Schematics of fabricated nanosandwiches for the detection of IL-6 [44]. Copyright 2017 American Chemical Society.

3.2 Nanomaterials as nanocatalysts

Recently, nanomaterials with excellent catalytic ability have been extensively exploited and applied in the biosensing fields owing to their high stability and low cost. Cao et al. fabricated a sensitive electrochemical immunosensor for IL-6 detection by using $NiCoO_2$@CeO_2 nanoboxes (NBs) as electrocatalysts to accelerate the oxygen evolution reaction (OER) in a neutral solution [49]. As illustrated in Figure 6, zeolitic imidazolate framework (ZIF-67) nanocubes were used as the templates to prepare $NiCoO_2$ NBs and then further decorated with CeO_2 NPs on the surface. Antibody was immobilized on the NPs based on the formation of ester-like linkage between CeO_2 and the carboxylic groups. Carboxylated graphene was used to functionalize the GCE for binding with antibody. $NiCoO_2$@CeO_2 NBs possessed higher OER activity than $NiCoO_2$ NBs, which is attributed to the synergistic effect between CeO_2 and $NiCoO_2$.

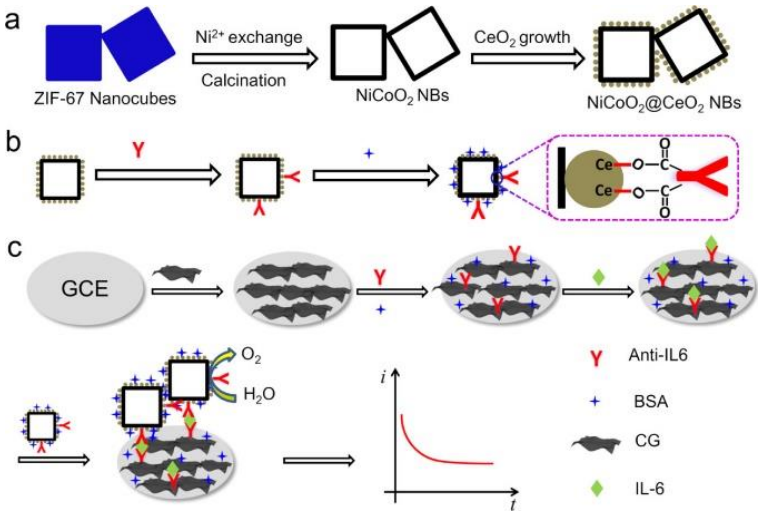

Figure 6. Illustration of the (a) synthesis procedure of $NiCoO_2$@CeO_2 NBs, (b) Preparation procedure of electrocatalytic labels, and (c) fabrication procedure of the immunosensor [49]. Copyright 2020 American Chemical Society.

Table 2. Analytical performances of various electrochemical biosensors for interleukin detection with nanomaterials as the signal reporters.

Signal label	**Target**	**Detection limit (fg/mL)**	**Linear range (ng/mL)**	**Ref.**
alkaline phosphatase	IL-1	5.2×10^{3}	1×10^{-2} ~ 0.2	[34]
supersandwich multienzyme-DNA	IL-6	50	2×10^{-4} ~ 2×10^{-2}	[35]
biotinylated diaphorase/neutravidin	IL-8	1×10^{3}	1×10^{-3} ~ 1×10^{3}	[36]
HRP-labeled MWCNTs	IL-6	500	5×10^{-4} ~ 5×10^{-3}	[37]
AuNPs-PDA-CNTs-HRP	IL-6	300	1×10^{-3} ~ 4×10^{-2}	[38]
OAMs-ACP-HRP	IL-6	0.32	1×10^{-5} ~ 90	[41]
Ag^{+}-PEI-AuNPs	IL-8	1	5×10^{-4} ~ 0.1	[42]
Fc-loaded porous polyelectrolyte	IL-6	1×10^{3}	2×10^{-3} ~ 20	[43]
GO-NB	IL-6	1×10^{3}	1×10^{-3} ~ 0.3	[44]

Cd^{2+}-PS	IL-17	50	1×10^{-4} ~ 1	[45]
Cd^{2+}-PS and Fc-PS	IL-6 and IL-17	500 and 1×10^{3}	1×10^{-3} ~ 1 and 0.002 ~ 1	[46]
AgNPs-TiP	IL-6	100	5×10^{-4} ~ 10	[47]
Cd^{2+}-PS	IL-6	100	1×10^{-5} ~ 1×10^{3}	[48]
MBs-HRP	IL-6 and IL-8	10	Not reported	[40]
$NiCoO_2$@CeO_2 NBs	IL-6	7	2.5×10^{-5} ~ 10	[49]
DNA-templated CdTe/CdS QDs	IL-8	3.36	5×10^{-6} ~ 5×10^{-3}	[50]
PS@PDA-AgNPs	IL-6	59	1×10^{-4} ~ 100	[51]

Abbreviation: HRP, horseradish peroxidase; MWCNTs, multiwall carbon nanotubes; AuNPs, gold nanoparticles; PDA, polydopamine; CNTs, carbon nanotubes; MBs, magnetic beads; OAMs, octahedral anatase mesocrystals; ACP, acid phosphatase; PEI, polyethylenimine; Fc, ferrocene; GO, graphene oxide; NB, Nile blue; PS, polystyrene sphere; NBs, nanoboxes; QDs, quantum dots; PS, polystyrene; AgNPs, silver nanoparticles; TiP, hollow titanium phosphate sphere; AgNPs, silver nanoparticles.

3.3 Electroactive nanomaterials as signal reporters

Quantum dots (QDs) have been widely utilized in versatile applications, such as biosensing, bioimaging and optical devices because of their excellent physiochemical capabilities. When being used as the electrochemical signal reporters, numerous metal ions in QDs can be released under the treatment of acid and then determined by anodic stripping voltammetry (ASV). For this view, Xu et al. successfully synthesized DNA-templated CdTe/CdS QDs and applied them as the reporters to sensitively detect IL-8 [50]. However, the involvement of toxic ions and oxidative acid significantly limits the applications of QDs-based bioassays. Nanomaterials with electroactive properties can be directly used as the signal probes without the acid dissolution steps, thus having aroused the wide interest in bioassays. For instance, Lou et al. developed a competitive electrochemical immunosensor for human IL-6 detection by using silver nanoparticles (AgNPs)-functionalized polystyrene NPs [51]. In this work, an electrically heated carbon electrode was employed as the biosensing platform and was then modified with the nanocomposites of electrochemically reduced graphene oxide and gold-palladium bimetallic nanoparticles (ERGO-AuPdNPs). After the competitive immunoreaction, AgNPs tethered on the electrode surface produced a sharp and well-defined voltammetric signal through the solid-state Ag/AgCl reaction.

4. MAGNETIC NANOMATERIAALS-ASSISTED DETECTION

Because of their facile manipulation under magnetic field, MBs have been broadly used in various applications, such as sample purification and biosensing [52]. Liu et al. established a flexible AuE array for multiplex detection of three biomarkers (prostate specific antigen, prostate specific membrane antigen, and IL-6) [53]. As illustrated in Figure 7, the primary antibody-modified MBs were modified on the nanoAu film electrode with the effect of magnet. Gold nanorods (AuNRs) were utilized to carry HRP and second antibody. After the immunoreaction, an obvious electrochemical signal from H_2O_2 reduction reaction was observed. Besides, Ojeda et al. reported a MBs-based electrochemical immunosensor for the detection of IL-6 with poly-HRP streptavidin conjugate as the label for signal

amplification [54]. Magnetic nanomaterials can also be integrated with other materials or techniques to paly multiple functions. For example, Tang et al. reported the Fe_3O_4 NPs@GO@molecularly imprinted polymer for IL-8 detection in saliva [55].

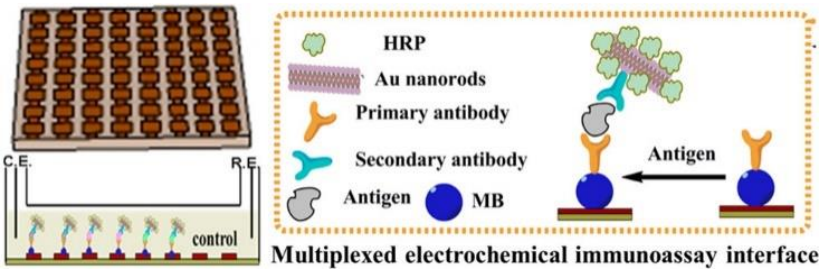

Figure 7. Illustration of preparation of the flexible microchip and the construction of multiplexed immunoassay interface [53]. Copyright 2014 American Chemical Society.

5. CONCLUSION

In this work, the development of nanomaterial-based electrochemical biosensors for the detection of different ILs was reviewed. Overall, nanomaterials exhibit excellent electrical activity and electrocatalytic property, providing a promising strategy to improve the sensitivity. However, there is still much room for improvement in the clinical applications of nanomaterials-based biosensors, especially in terms of repeatability and long-term stability. Moreover, the design of a biosensor capable of determining multiple biomarkers at the same time is desired. Due to the availability of non-invasive body fluids, especially saliva, the portable integrated electrochemical devices with high accuracy and reliability are desired for practical applications.

ACKOWLEDGMENTS
This work was supported by the Science & Technology Foundation of Yongzhou (2021-YZKJZD-018) and the Program for Innovative Research Team of Science and Technology in the University of Henan Province (21IRTSTHN005).

References

1. D. Kim and S. Taleban, *Drug Aging*, 325 (2019) 607.
2. H. Schmitt, M. F. Neurath and R. Atreya, *Front. Immunol.*, 12 (2021) 622934.
3. N. K. Bakirhan, G. Ozcelikay and S. A. Ozkan, *J. Pharm. Biomed. Anal.*, 159 (2018) 406.
4. M. A. Khan and M. Mujahid, *Sensors*, 20 (2020) 646.
5. J. Kim, S. Noh, J. A. Park, S.-C. Park, S. J. Park, J.-H. Lee, J.-H. Ahn and T. Lee, *Sensors*, 21 (2021) 8491.
6. F. Ding and X. Li, *Int. J. Electrochem. Sci.*, 12 (2017) 11646.

7. T. Sun, Y. Guo and F. Zhao, *Int. J. Electrochem. Sci.*, 16 (2021) 210732.
8. X. Ma, *Int. J. Electrochem. Sci.*, 15 (2020) 7663.
9. C. Russell, A. C. Ward, V. Vezza, P. Hoskisson, D. Alcorn, D. P. Steenson and D. K. Corrigan, *Biosens. Bioelectron.*, 126 (2019) 806.
10. E. B. Aydin and M. K. Sezginturk, *Bioelectrochemistry*, 138 (2021) 107698.
11. E. B. Aydin and M. K. Sezginturk, *Anal Chim Acta*, 1039 (2018) 41.
12. E. B. Aydin and M. K. Sezginturk, *Anal. Biochem.*, 554 (2018) 44.
13. R. Sharma, S. E. Deacon, D. Nowak, S. E. George, M. P. Szymonik, A. A. S. Tang, D. C. Tomlinson, A. G. Davies, M. J. McPherson and C. Walti, *Biosens. Bioelectron.*, 80 (2016) 607.
14. E. B. Aydın and M. K. Sezgintürk, *Electroanalysis*, 33 (2021) 1596.
15. D. Gentili, P. D'Angelo, F. Militano, R. Mazzei, T. Poerio, M. Brucale, G. Tarabella, S. Bonetti, S. L. Marasso, M. Cocuzza, L. Giorno, S. Iannotta and M. Cavallini, *J Mater Chem B*, 6 (2018) 5400.
16. E. B. Aydın, M. Aydın and M. K. Sezgintürk, *Sens. Actuat. B: Chem.*, 270 (2018) 18.
17. A. Garcia-Cruz, F. Nessark, M. Lee, N. Zine, M. Sigaud, R. Pruna, M. Lopez, P. Marote, J. Bausells, N. Jaffrezic-Renault and A. Errachid, *Sens. Actuat. B: Chem.*, 255 (2018) 2520.
18. E. B. Aydin, *Talanta*, 215 (2020) 120909.
19. F. Nessark, M. Eissa, A. Baraket, N. Zine, B. Nessark, A. Zouaoui, J. Bausells and A. Errachid, *Electroanalysis*, 32 (2020) 1795.
20. E. B. Aydin, M. Aydin and M. K. Sezginturk, *Talanta*, 222 (2021) 121596.
21. M. d. L. Gonçalves, L. A. N. Truta, M. G. F. Sales and F. T. C. Moreira, *Anal. Lett.*, 54 (2021) 2611.
22. E. B. Aydın, M. Aydın and M. K. Sezgintürk, *New J. Chem.*, 44 (2020) 14228.
23. A. R. Cardoso, M. H. de Sa and M. G. F. Sales, *Bioelectrochemistry*, 130 (2019) 107287.
24. J. Sabate Del Rio, O. Y. F. Henry, P. Jolly and D. E. Ingber, *Nat. Nanotechnol.*, 14 (2019) 1143.
25. C. Deng, F. Qu, H. Sun and M. Yang, *Sens. Actuat. B: Chem.*, 160 (2011) 471.
26. Z. Wang, S. Yang, Y. Wang, W. Feng, B. Li, J. Jiao, B. Han and Q. Chen, *Anal. Chim. Acta*, 1140 (2020) 145.
27. K. Parate, S. V. Rangnekar, D. Jing, D. L. Mendivelso-Perez, S. Ding, E. B. Secor, E. A. Smith, J. M. Hostetter, M. C. Hersam and J. C. Claussen, *ACS Appl. Mater. Interfaces*, 12 (2020) 8592.
28. M. Tertiş, B. Ciui, M. Suciu, R. Săndulescu and C. Cristea, *Electrochim. Acta*, 258 (2017) 1208.
29. M. Tertis, P. I. Leva, D. Bogdan, M. Suciu, F. Graur and C. Cristea, *Biosens. Bioelectron.*, 137 (2019) 123.
30. N. Pachauri, G. Lakshmi, S. Sri, P. K. Gupta and P. R. Solanki, *Mater. Sci. Eng. C*, 113 (2020) 110911.
31. T. Yang, S. Wang, H. Jin, W. Bao, S. Huang and J. Wang, *Sens. Actuat. B: Chem.*, 178 (2013) 310.
32. S. Verma, A. Singh, A. Shukla, J. Kaswan, K. Arora, J. Ramirez-Vick, P. Singh and S. P. Singh, *ACS Appl. Mater. Interfaces*, 9 (2017) 27462.
33. Z. Liu, Q. Huang, J. Chen, J. Yao, M. Jin, X. Wang, E. M. Akinoglu, M. Zhang, N. Li and L. Shui, *J. Electroanal. Chem.*, 883 (2021) 115068.
34. S. Guerrero, L. Agui, P. Yanez-Sedeno and J. M. Pingarron, *Bioelectrochemistry*, 133 (2020) 107484.
35. G. Wang, H. Huang, B. Wang, X. Zhang and L. Wang, *Chem. Commun.*, 48 (2012) 720.
36. A. Bhatia, H. S. Na, P. Nandhakumar, B. Yu, S. Jon, J. Chung and H. Yang, *Sens. Actuat. B: Chem.*, 326 (2021) 128979.
37. R. Malhotra, V. Patel, J. P. Vaque, J. S. Gutkind and J. F. Rusling, *Anal. Chem.*, 82 (2010) 3118.
38. G. Wang, X. He, L. Chen, Y. Zhu and X. Zhang, *Colloid. Surf. B*, 116 (2014) 714.
39. C. K. Tang, A. Vaze, M. Shen and J. F. Rusling, *ACS Sens.*, 1 (2016) 10363.
40. R. Malhotra, V. Patel, B. V. Chikkaveeraiah, B. S. Munge, S. C. Cheong, R. B. Zain, M. T.

Abraham, D. K. Dey, J. S. Gutkind and J. F. Rusling, *Anal. Chem.*, 84 (2012) 6249.
41. N. Liu, H. Yi, Y. Lin, H. Zheng, X. Zheng, D. Lin and H. Dai, *Microchim. Acta*, 185 (2018) 277.
42. T. Putnin, A. Ngamaroonchote, N. Wiriyakun, K. Ounnunkad and R. Laocharoensuk, *Microchim. Acta*, 186 (2019) 305.
43. T. Li and M. Yang, *Sens. Actuat. B: Chem.*, 158 (2011) 361.
44. M. Qi, J. Huang, H. Wei, C. Cao, S. Feng, Q. Guo, E. M. Goldys, R. Li and G. Liu, *ACS Appl. Mater. Interfaces*, 9 (2017) 41659.
45. W. Jiang, T. Li, F. Qu, L. Ding, Z. Shen and M. Yang, *Sens. Actuat. B: Chem.*, 185 (2013) 658.
46. T. Li, B. Shu, B. Jiang, L. Ding, H. Qi, M. Yang and F. Qu, *Sens. Actuat. B: Chem.*, 186 (2013) 768.
47. J. Peng, L. N. Feng, Z. J. Ren, L. P. Jiang and J. J. Zhu, *Small*, 7 (2011) 2921-2928.
48. J. J. Shi, T. T. He, F. Jiang, E. S. Abdel-Halim and J. J. Zhu, *Biosens. Bioelectron.*, 55 (2014) 51.
49. L. Cao, J. Cai, W. Deng, Y. Tan and Q. Xie, *Anal. Chem.*, 92 (2020) 16267.
50. J. Xu, X. Yu, L. Xie and M. Shao, *Anal. Bioanal. Chem.*, 412 (2020) 2599.
51. Y. Lou, T. He, F. Jiang, J. J. Shi and J. J. Zhu, *Talanta*, 122 (2014) 135.
52. J. Min, M. Nothing, B. Coble, H. Zheng, J. Park, H. Im, G. F. Weber, C. M. Castro, F. K. Swirski, R. Weissleder and H. Lee, *ACS Nano*, 12 (2018) 3378.
53. J. Liu, C. Y. Lu, H. Zhou, J. J. Xu and H. Y. Chen, *ACS Appl. Mater. Interfaces*, 6 (2014) 20137.
54. I. Ojeda, M. Moreno-Guzman, A. Gonzalez-Cortes, P. Yanez-Sedeno and J. M. Pingarron, *Anal. Bioanal. Chem.*, 406 (2014) 6363.
55. P. Tang, H. Zhang, J. Huo and X. Lin, *Anal. Methods*, 7 (2015) 7784.